

Temperature Effect on Buckling Properties of Thin-Walled Composite Profile Subjected to Axial Compression

Katarzyna Falkowicz^{1*}, Michał Kuciej², Łukasz Świąch³

¹ Faculty of Mechanical Engineering, Department of Machine Design and Mechatronics, Lublin University of Technology, ul. Nadbystrzycka 36, 20-618 Lublin, Poland

² Faculty of Mechanical Engineering, Department of Organisation of Enterprise, Białystok University of Technology, ul. Wiejska 45C, 15-351 Białystok, Poland

³ Faculty of Mechanical Engineering and Aeronautics, Department of Aerospace Engineering, Rzeszów University of Technology, aleja Powstańców Warszawy 12, 35-959 Rzeszów, Poland

* Corresponding author's e-mail: k.falkowicz@pollub.pl

ABSTRACT

This study investigates the influence of temperature variations on the buckling properties of thin-walled omega-profiles fabricated from carbon-epoxy composite materials. Utilizing a MTS testing machine, compression tests were conducted on these profiles at temperatures ranging from -20°C to 80°C , in 20°C increments. The primary objective was to assess how temperature fluctuations impact the buckling load and load-bearing capacity of these composite profiles under axial compression. The experimental setup allowed for precise measurement of load-displacement and load-deflection characteristics, and the critical load at which buckling initiation occurred. Observations revealed that the buckling resistance of the profiles exhibited a complex dependence on temperature. At lower temperatures, the composite material demonstrated enhanced stiffness and strength, marginally increasing buckling resistance. Conversely, at elevated temperatures, a noticeable degradation in mechanical properties was observed, leading to a reduced buckling load and altered failure modes. To complement the experimental findings, a comprehensive finite element (FE) analysis was conducted for sample in room temperature. The FE model, developed to replicate the experimental conditions closely, employed an eigenvalue-based approach to predict the buckling initiation and progression accurately. The presented results are the results of only preliminary tests and they will be expand about more samples number as well as to determine material properties for various temperatures.

Keywords: temperature effect, finite element method, composite, buckling.

INTRODUCTION

In recent years, composite materials have gained prominence in various engineering fields due to their exceptional properties such as high strength and stiffness coupled with lightweight, especially in aerospace [1–4], building industry [5, 6] or medicine. Among the numerous examples of contemporary applications of composite structures are wind turbine blades [7], pipelines, industrial tanks or chimney structures [8, 9]. In view of such a wide spectrum of applications, these structures can be subjected to different types of impacts, i.e. mechanical, chemical but

also thermal loading, which is the focus of this paper. The influence of temperature can therefore be crucial for some structures and lead to effects such as: loss of stability [10–13], material degradation [14, 15], degradation of elastic constants, delamination [14, 16–18], reinforcement slippage, creep, thermal flow. It is also worth mentioning that already during the manufacturing process, composites are subjected to increased temperatures [19], and then cooled to ambient temperature, which can lead to residual stresses in the material [20]. The subject matter of this paper, however, relates to the problem of stability [21–24]. As is known from the literature and research

carried out, stability depends on factors such as boundary conditions [25–27], stiffness related to material characteristics, including the orientation of fibres in layers in the case of laminates [28–31]. Imperfections, i.e. imperfections of various kinds, which can be related to geometry [32–34], loading mode, stiffness distribution or boundary conditions, also play a very important role.

One of the most relevant review papers dealing with the problem of temperature effects on composite sandwich structures is that of Noor and Burton [16]. In this work, articles addressing, among other topics, the stability of thermally loaded composite sandwich panels and shells were tabulated. In paper [35] authors tested buckling behaviour of lenticular collapsible composite tube subjected to axial compression at three different temperatures and they got good agreement between experimental and numerical results. Paper [36] deeply studies the temperature effect on buckling behavior of prestressed CFRP-reinforced steel columns. They tested samples in two temperature situations: when the column was loaded at a certain temperature and when the column is preloaded and then the temperature changes. For first situation the buckling capacity maintains almost constant with temperature from 20°C to 80°C and increase 3–7% for temperature under 20°C. For second situation column extends, and the deformation is first symmetric and global and then changes to local and asymmetric when the temperature reaches a turning point, and under 20°C, the column shrinks, and the deformation is symmetric and global. Tauchert et al. studied the thermal buckling behavior of thin and thick antisymmetric angle-ply rectangular plates [37].

However, the behaviour of these materials under different temperature ranges, especially in the context of compressing thin-walled omega-profiles, remains an area requiring deeper understanding. This study focuses on the experimental analysis of the temperature effect on the mechanical properties of thin-walled omega-profiles made of carbon-epoxy composite under compression. Experimental tests were carried out using a testing machine equipped with a thermal chamber and cooling system and the Aramis optical system. Experiments were conducted across a wide temperature range, from -20°C to 80°C at 20-degree intervals, to understand how material behaviour changes under different thermal conditions. Moreover, to complement the experimental findings, a comprehensive finite element analysis

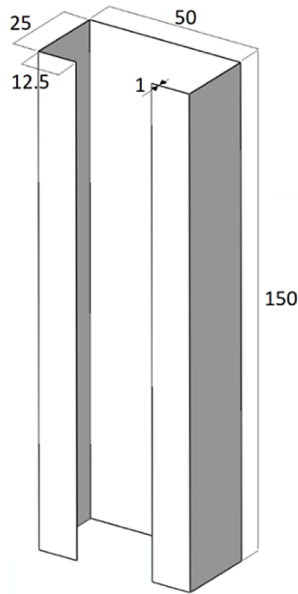
was conducted for sample in room temperature. The experiments revealed significant differences in material behaviour depending on the temperature, highlighting the impact of thermal conditions on the strength of carbon-epoxy composites. These findings are crucial for the design and optimization of structural elements used in sectors where materials are exposed to diverse temperature ranges, such as aviation, automotive, or renewable energy.

This paper and presented here analysis of experimental results provides new insights into the degradation mechanisms and behaviour of carbon-epoxy composites under thermal conditions, which may contribute to a better understanding and prediction of their long-term strength and reliability.

RESEARCH SUBJECT AND METHODOLOGY

The investigation focused on a open cross-section omega made of carbon-epoxy composite. The geometric parameters and stacking sequence of specimens used in tests is shown in Figure 1. The specimen were made of CFRP (ang. *Carbon-Fiber Reinforced Polymer*) composite material, characterized by anisotropic mechanical properties like: a longitudinal Young's modulus $E_1 = 118.32$ GPa, a transverse Young's modulus $E_2 = 7.05$ GPa, a Poisson's ratio $\nu_{12} = 0.32$, a shear modulus $G_{12} = 3.25$ GPa. The material mechanical properties were determined according to ISO standards. All specimens had the same thickness of 1mm and an-symmetrical stacking sequence. Chosen stacking sequence configuration is characterized by Hygro-Thermally Curvature Stable properties. More information about the HTCS and coupled laminates can be found in the articles [38–42]. The specimen were made by autoclave method.

The axial compression tests were performed on servo-hydraulic MTS (ang. *Materials Test Systems*) testing machine in wide temperature range, from -20°C to 80°C in average of 20-degree intervals and with continuous displacement rate of 1 mm/min. Figures 2a, 2b and 2c detail the apparatus for temperature regulation, incorporating a heating mechanism for achieving a maximum temperature of 80°C, and a cooling system, utilizing liquid nitrogen, to reach a minimum temperature of -20°C. During the test recorded the load-displacement curves from machine and load-deflection curves from GOM ARAMIS system based on 3D Digital Image Correlation (DIC)



Specimen	Configuration
PNI	[60/0/-60 ₂ /0/60/0/90 ₂ /0]

Fig. 1. Geometry and dimension of tested samples

method [43, 44] at each temperature and observed buckling behaviour. The boundary conditions of samples in test present in Figure 2a. Moreover, for reference temperature, a numerical analysis was performed in order to compare the results obtained in the experimental studies.

RESULTS AND DISCUSSION

During the test, the shortening of the specimens and the deflection in the direction perpendicular to the plane of the profile wall were recorded for each temperature considered. Figure 3 shows the working

paths obtained from the machine for all the temperatures tested. Figure 4, on the other hand, shows an example of the deflection characteristics for a selected specimen at -20 °C, for three different points. From the graphs shown, we can see the significant effect of temperature on the operation of the tested profiles. Moreover, Figure 4 confirms that the selection of a point for displacement analysis is of great importance, and that by selecting a point from a different half-wave we can obtain different characteristics. Therefore, the selection of points is quite important.

Since the identification of failure loads is notably straightforward due to the specimens' abrupt breakage, the identification of buckling initiation load is more complicated. The $P-w^2$ approximation method was used to estimate the value of the critical load on the basis of the obtained results of measurements carried out during the implementation of the experimental tests. In this method, the critical load is determined on the basis of the postcritical equilibrium path, however, the estimation of the approximate value of the critical force is based on the characteristics of the load with respect to the square of the deflection measured in the direction perpendicular to the plane of the profile wall. In the present study, the value of deflection w was obtained from the deflection measurement recorded with DIC. The covered equilibrium path $P-w^2$ was approximated by a linear function of the form [45]:

$$P = P_{cr} \frac{a_1}{a_0} w + P_{cr} \quad (1)$$

where: a_0, a_2 – the parameters of the function, P – the value of the loading force, P_{cr} – the value of the unknown critical load, while w^2 is the square of the increase in deflection measured perpendicular to the profile wall.

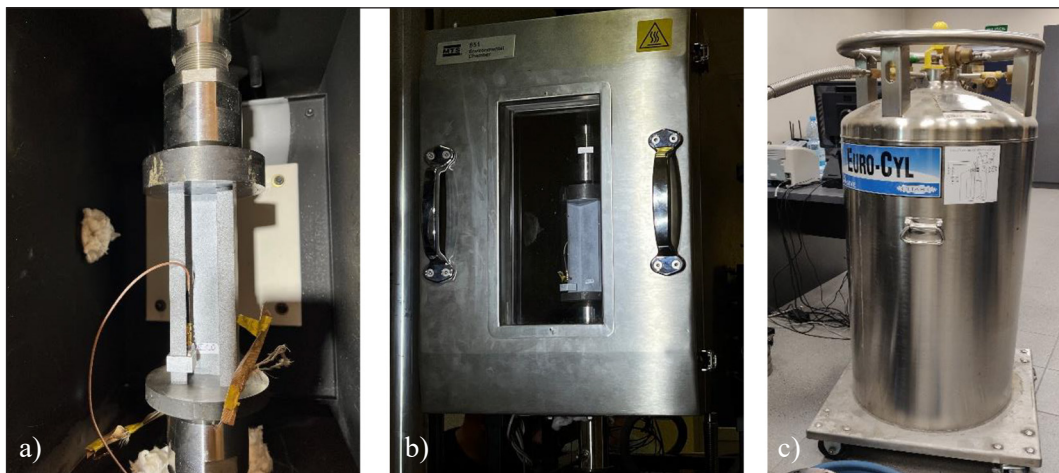


Fig. 2. Test stand: (a) mounted sample, (b) high temperature stand, (c) liquid nitrogen to low temperature system

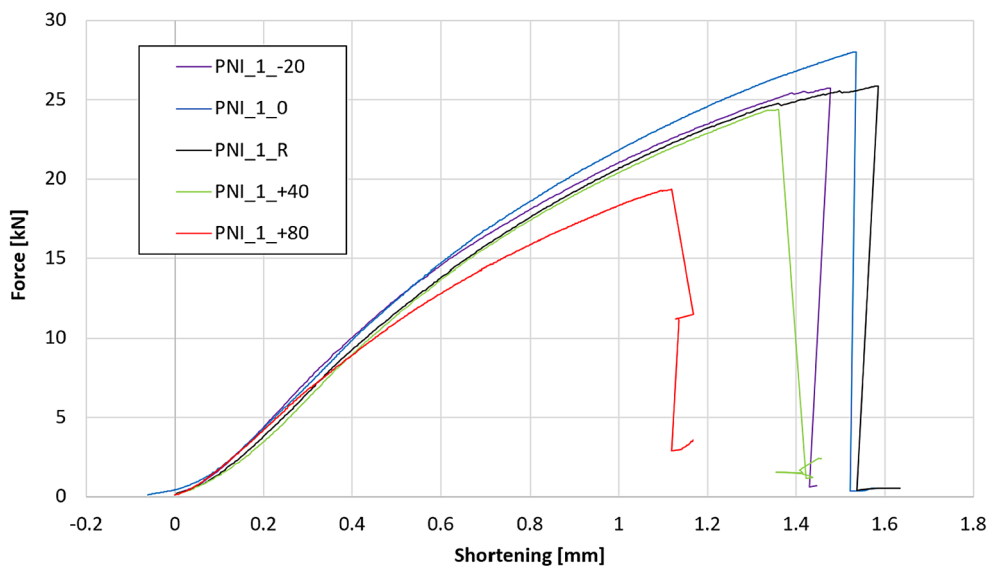


Fig. 3. Load-shortening curves of tested omega profiles from Instron machine for all temperatures

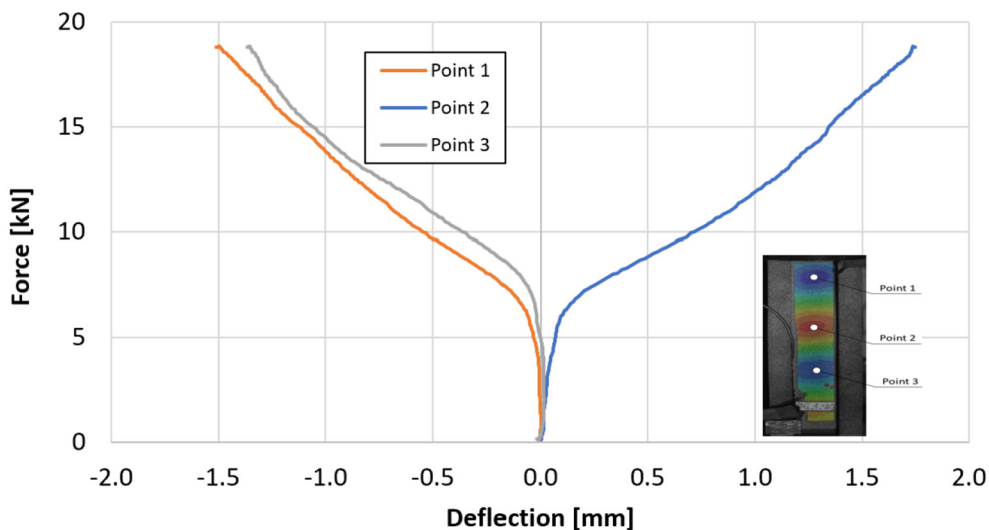


Fig. 4. Exemplary load-deflection curves of tested omega profiles from DIC system for PI_-20 sample

The critical load in this case is defined as the point of intersection of the approximation function with the vertical axis of the coordinate system of the postcritical $P-w^2$ structure characteristic. The method is described in detail in papers [45]. Examples of approximation characteristics for selected cases of the test samples are shown in Figure 5. Blue color lists the value of critical force. The approximation method was carried out for the characteristics determined for point 1. Based on the paths presented in Figure 6 buckling loads have been calculated and summarized in Table 1 and in Figure 6. We can observe significant impact of temperature on buckling load value. Comparatively, the buckling load at a cooler temperature of -20°C is close to the reference

temperature (room temperature of 20°C). Conversely, at a higher temperature of 80°C , there's a marked reduction of 22% from the reference, underscoring a substantial decline in the capacity to withstand buckling. Comparison, the highest critical force value was obtained at 0°C – 8% higher than the reference temperature.

Furthermore, in order to verify the experimental studies, a numerical analysis was carried out for a reference temperature. The calculations were carried out in Abaqus program, (using very popular and widely used finite element method [46–52], by solving a linear eigenvalue based on the minimum potential energy criterion of the system. The FE model with boundary conditions and buckling form present in Figure 7.

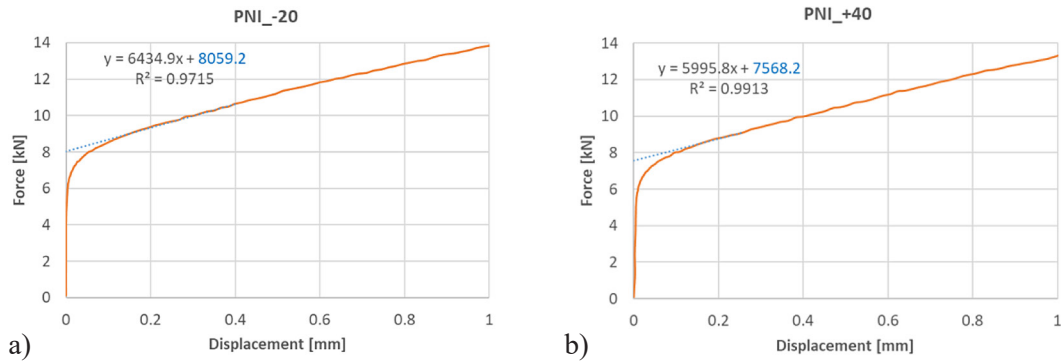


Fig. 5. Approximate critical force values for selected cases of omega columns: (a) -20°C, (b) +40°C

Table 1. Experimental results of buckling load (point 1)

Critical force	Temperature	Different according to the reference temp. (20°C)
[N]	[C°]	[%]
8 059.20	-20	-5
9 133.70	0	+8
8 456.80	+20	0
7 568.20	+40	-11
6 588.70	+80	-22

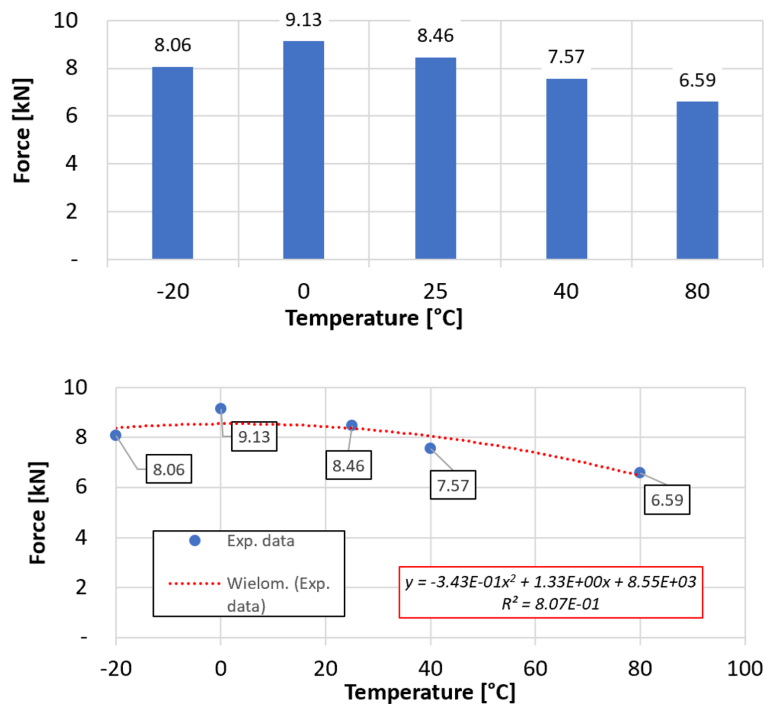


Fig. 6. Critical force (P_{cr}) vs temperature

The boundary conditions defined for the numerical model were an adequate representation of the experimental tests. The discrete model of the omega column was based in both end sections on rigid plates, for which the boundary conditions, were defined at reference points assigned to each

plate. The bottom plate was fully restrained by locking all degrees of freedom at the reference point, while the top plate was left with the exclusive possibility of moving in the direction of the compression load realization, i.e. along the longitudinal axis of the column (Z axis). The

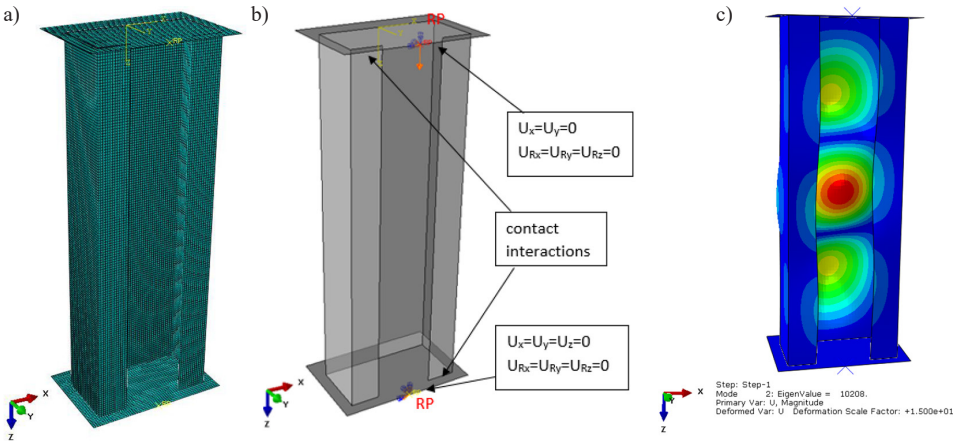


Fig. 7. FE model: (a) discrete model, (b) boundary conditions, (c) buckling form from Abaqus in +20°C

compression load was realized by displacing the top plate in the direction of the Z axis. The edges of the column end sections were freely supported by the surfaces of the non-deformable plates, where, in addition, contact interactions were defined at the interface between the edge and the plate surface. The composite structure was mapped by the thickness of the shell element, using the so-called Layup-Ply technique. In the developed numerical

model for a single laminate layer, an orthotropic material model in the plane stress state was defined, assuming the experimentally determined mechanical properties of the composite material. SHELL-type elements were used in the discretization of the composite column. The composite structure consisted of SC8R-type finite elements. In addition, non-deformable shell elements with a linear shape function - R3D4 - were used in the

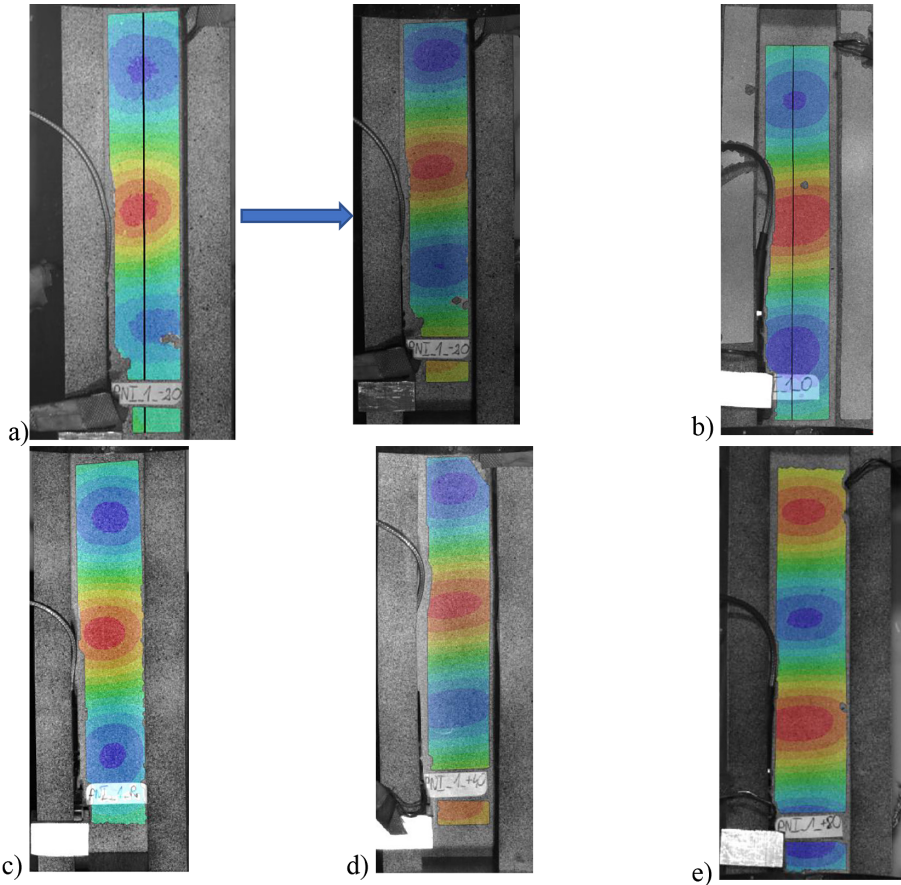


Fig. 8. Buckling form under axial compression: (a) -20°C, (b) 0°C, (c) 20°C, (d) 40°C, (e) 80°C

numerical model, applied to discretize the sub-assemblies constituting the rigid column supports. In the developed numerical models adopted a uniform finite element mesh in which the dimension of a single shell element was 1x1mm. The discrete model developed was composed of 23700 finite elements (18900 - column, 4800 - plates).

It can be observed that experimental findings indicate a lower threshold for buckling initiation compared to numerical predictions, the critical value obtained in FEM simulations was 17% higher than that obtained from experimental tests. It can be stemming from notable alterations in the structural rigidity observed during testing. Subtle factors, such as imperceptible slippage and deviations from ideal simply supported scenarios, can markedly impact the rigidity of the structure in practice. Conversely, the numerical simulations assume idealized boundary conditions, leading to higher predicted values than those recorded in physical experiments.

In Figure 8 present recorded buckling form by 3D DIC system for all tested samples in considered temperatures. During the experimental tests, it was observed that for different temperatures there were specific numbers of half-waves in the longitudinal direction of the column: -20°C – at the beginning three half-waves and then four half-waves, 0°C – three half-waves, $+20^{\circ}\text{C}$ – three half-waves, $+40^{\circ}\text{C}$ – four half-waves and $+80^{\circ}\text{C}$ – four half-waves. Moreover, it can be seen, that numerical buckling form for PNI_+20 sample (Figure 8c), correlates well with experimental observations (Figure 7c). It can be seen that at lower temperatures, the composite material demonstrated enhanced stiffness and strength, marginally increasing buckling resistance. Conversely, at elevated temperatures, a noticeable degradation in mechanical properties was observed, leading to a reduced buckling load and altered failure modes.

CONCLUSIONS

This research investigated the experimental studies on the temperature effect on buckling behaviour of thin-walled composite profile subjected to axial compression. In addition, for verification purposes, a numerical analysis was carried out for a compression specimen at a reference temperature. From the results obtained, a significant effect of temperature on the critical force can be seen. The buckling load, on average, is about 8% greater at 0°C than at 20°C , whereas that is

about 22% lower at 80°C than at 20°C . Comparatively, the buckling load at a cooler temperature of -20°C is close to the reference temperature. The buckling modes for samples at reference temperature, predicted from FE analysis correlate well with the experimental observations, only the critical force value is 17% higher compared to experiment. However, it should be borne in mind that inaccuracies of all kinds occurring during the experimental studies, caused by various independent factors such as geometrical imperfections of the structure or the way the load and boundary conditions are implemented, make it difficult to accurately determine the critical load value of the thin-walled structure. In addition, the experimental critical force values were determined on the basis of a single approximation method adopted. Therefore, the determined values of critical forces are approximate values. In addition, it should be emphasized here that the results presented are the results of preliminary tests carried out on one series of specimens. The research should be extended to include a larger number of specimens and the determination of material properties at different temperatures in order to compare the results obtained using the numerical method, as well as the determination of critical forces using other approximation methods [53–55]. What is more, for prediction of buckling behaviour the artificial neural networks (ANNs) could be used [56]. Summarize, this study opens new perspectives for further research on optimizing carbon-epoxy composites for applications requiring high resistance to variable temperature conditions.

Acknowledgments

The research leading to these results has received funding from the commissioned task entitled “VIA CARPATIA Universities of Technology Network named after the President of the Republic of Poland Lech Kaczyński” contract no. MEiN/2022/DPI/2575 action entitled “In the neighborhood – inter-university research internships and study visits.”

REFERENCES

1. Puig L., Barton A., Rando N. A review on large deployable structures for astrophysics missions. *Acta Astronautica*. 2010; 67(1–2): 12–26.
2. Kopecki T., Mazurek P., Lis T. Experimental and Numerical Analysis of a Composite Thin-Walled

- Cylindrical Structures with Different Variants of Stiffeners, Subjected to Torsion. *Materials*. 2 października 2019; 12(19): 3230.
3. Czyż Z, Podolak P, Skiba K, Jakubczak P, Karpiński P, Różyło P, i in. Autogyro Main Rotor Blade Strength Tests. In: 2023 IEEE 10th International Workshop on Metrology for AeroSpace (MetroAeroSpace) [Internet]. Milan, Italy: IEEE; 2023; 199–204. Available at: <https://ieeexplore.ieee.org/document/10190031/>
 4. Kopecki H, Świąch Ł. Experimental investigation of limit load of composite sandwich plate with cut-out. In: Pietraszkiewicz W, Witkowski W, (Eds.). *Shell Structures: Theory and Applications Volume 4* [Internet]. 1. wyd. CRC Press; 2017; 425–8. Available at: <https://www.taylorfrancis.com/books/9781351680486/chapters/10.1201/978135166605-97>
 5. Chróścielewski J, Miśkiewicz M, Pyrzowski Ł, Rucka M, Sobczyk B, Wilde K. Modal properties identification of a novel sandwich footbridge – Comparison of measured dynamic response and FEA. *Composites Part B: Engineering*. 2018; 151: 245–55.
 6. Chróścielewski J, Miśkiewicz M, Pyrzowski Ł, Sobczyk B, Wilde K. A novel sandwich footbridge - Practical application of laminated composites in bridge design and in situ measurements of static response. *Composites Part B: Engineering*. 2017; 126: 153–61.
 7. Tamayo-Avenida JM, Patiño-Arcila ID, Nieto-Londoño C, Sierra-Pérez J. Fluid-structure interaction analysis of a wind turbine blade with passive control by bend-twist coupling. *Energies*. 2023; 16(18): 6619.
 8. Mikhail AE, El Damatty AA. Non-linear analysis of FRP chimneys under thermal and wind loads. *Thin-Walled Structures*. 1999; 35(4): 289–309.
 9. El Damatty AA, Awad AS, Vickery BJ. Thermal analysis of FRP chimneys using consistent laminated shell element. *Thin-Walled Structures*. 2000; 37(1): 57–76.
 10. Ko L. Predictions of Thermal Buckling Strengths of Hypersonic Aircraft Sandwich Panels Using Minimum Potential Energy and Finite Element Methods. 1995.
 11. Wysmulski P. Load Eccentricity of compressed composite z-columns in non-linear state. *Materials*. 2022; 15(21): 7631.
 12. Falkowicz K, Debski H. The post-critical behaviour of compressed plate with non-standard play orientation. *Composite Structures*. 2020; 252: 112701.
 13. Golewski P, Sadowski T, Kneć M, Budka M. The effect of thermal aging degradation of CFRP composite on its mechanical properties using destructive and non-destructive methods and the DIC system. *Polymer Testing*. 2023; 118: 107902.
 14. Dimitrienko YuI. Thermomechanical behaviour of composite materials and structures under high temperatures: 1. *Materials. Composites Part A: Applied Science and Manufacturing*. 1997; 28(5): 453–61.
 15. Hu C, Xu Z, Qiu J, Wu S, Wang R, He X. A unified modeling strategy of the stability and progressive damage behavior of CFRP double-blade composite stiffened structures (DCSS) under uniaxial compression. *Thin-Walled Structures*. 2023; 189: 110896.
 16. Noor AK, Burton WS. Computational models for high-temperature multilayered composite plates and shells. *Applied Mechanics Reviews*. 1992; 45(10): 419–46.
 17. Uematsu Y, Kitamura T, Ohtani R. Delamination behavior of a carbon-fiber-reinforced thermoplastic polymer at high temperatures. *Composites Science and Technology*. 1995; 53(3): 333–41.
 18. Rzeczkowski J, Samborski S, Valvo PS. Effect of stiffness matrices terms on delamination front shape in laminates with elastic couplings. *Composite Structures*. 2020; 233: 111547.
 19. Tompkins SS. Thermal expansion of selected graphite reinforced polyimide-, epoxy-, and glass-matrix composite.
 20. Gotsis PK, Guptill JD. Fiber composite thin shells subjected to thermal buckling loads. *Computers & Structures*. 1994; 53(6): 1263–74.
 21. Falkowicz K. Experimental and numerical failure analysis of thin-walled composite plates using progressive failure analysis. *Composite Structures*. 2023; 305: 116474.
 22. Falkowicz K. Numerical Investigations of perforated CFRP Z-cross-section profiles, under axial compression. *Materials*. 2022; 15(19): 6874.
 23. Kubit A, Świąch Ł, Trzepieciński T, Faes K. Experimental analysis of the post-buckling behaviour of compressed stiffened panel with refill friction stir spot welded and riveted stringers. *Adv Sci Technol Res J*. 2022; 16(2): 159–67.
 24. Rozyło P, Debski H. Stability and load carrying capacity of thin-walled composite columns with square cross-section under axial compression. *Composite Structures*. 2024; 329: 117795.
 25. Sabik A, Kreja I. Numerical analysis of laminated shells under in-plane axial compression. *Proc Appl Math and Mech*. 2009; 9(1): 251–2.
 26. Al-Hassani STS, Darvizeh M, Haftchenari H. An analytical study of buckling of composite tubes with various boundary conditions. *Composite Structures*. 1997; 39(1–2): 157–64.
 27. Wysmulski P, Teter A, Debski H. Effect of load eccentricity on the buckling of thin-walled laminated C-columns. W Lublin, Poland; 2018; 080008. Available at: <https://pubs.aip.org/aip/acp/article/608531>
 28. Pietraszkiewicz W, Kreja I, redaktorzy. *Shell Structures: Theory and Applications (Vol. 2): Proceedings of the 9th SSTA Conference, Jurata, Poland, 14-16 October 2009* [Internet]. CRC Press; 2009. Available at: <http://www>.

- rcnetbase.com/doi/book/10.1201/9780203859766
29. Kubiak T, Urbaniak M, Kazmierczyk F. The influence of the layer arrangement on the distortional post-buckling behavior of open section beams. *Materials*. 2020; 13(13): 3002.
 30. Falkowicz K, Debski H. Stability analysis of thin-walled composite plate in unsymmetrical configuration subjected to axial load. *Thin-Walled Structures*. 2021; 158: 107203.
 31. Falkowicz K, Valvo P. Influence of composite lay-up on the stability of channel-section profiles weakened by cut-outs – a numerical investigation. *Adv Sci Technol Res J*. 2023; 17(1): 108–15.
 32. Falkowicz K. Effect of cut-out radius for behaviour of symmetrically laminated plates. *J Phys: Conf Ser*. 2021; 1736: 012030.
 33. Rozylo P, Rogala M, Pasnik J. Buckling analysis of thin-walled composite structures with rectangular cross-sections under compressive load. *Materials*. 2023; 16(21): 6835.
 34. Banat D, Mania R. Failure analysis of thin-walled GLARE members during buckling and post-buckling response. W Zakopane, Poland; 2019; 020001. Available at: <https://pubs.aip.org/aip/acp/article/736694>
 35. Bai J, Xiong J. Temperature effect on buckling properties of ultra-thin-walled lenticular collapsible composite tube subjected to axial compression. *Chinese Journal of Aeronautics*. 2014; 27(5): 1312–7.
 36. Hu L, Liang X, Feng P, Li HT. Temperature effect on buckling behavior of prestressed CFRP-reinforced steel columns. *Thin-Walled Structures*. 2023; 188: 110879.
 37. Tauchert TR. Thermal buckling of thick antisymmetric angle-ply laminates. *Journal of Thermal Stresses*. 1987; 10(2): 113–24.
 38. York CB, Lee KK. Test validation of extension-twisting coupled laminates with matched orthotropic stiffness. *Composite Structures*. 2020; 242: 112142.
 39. York CB. Tapered hygro-thermally curvature-stable laminates with non-standard ply orientations. *Composites Part A: Applied Science and Manufacturing*. 2013; 44: 140–8.
 40. Falkowicz K. Validation of extension-bending and extension-twisting coupled laminates in elastic element. *Adv Sci Technol Res J*. 2023; 17(3): 309–19.
 41. Falkowicz K, Debski H, Wysmulski P. Effect of extension-twisting and extension-bending coupling on a compressed plate with a cut-out. *Composite Structures*. 2020; 238: 111941.
 42. Cross RJ, Haynes RA, Armanios EA. Families of hygrothermally stable asymmetric laminated composites. *Journal of Composite Materials*. 2008; 42(7): 697–716.
 43. Lusiak T, Kneć M. Use of ARAMIS for fatigue process control in the accelerated test for composites. *transportation research procedia*. 2018; 35: 250–8.
 44. Charchalis A, Kneć M, Żuk D, Abramczyk N. Use of 3D optical techniques in the analysis of the effect of adding rubber recyclate to the matrix on selected strength parameters of epoxy-glass composites. *Acta Mechanica et Automatica*. 2023; 17(3): 333–46.
 45. Paszkiewicz M, Kubiak T. Selected problems concerning determination of the buckling load of channel section beams and columns. *Thin-Walled Structures*. 2015; 93: 112–21.
 46. Jonak J, Karpiński R, Wójcik A. Numerical analysis of undercut anchor effect on rock. *J Phys: Conf Ser*. 2021; 2130(1): 012011.
 47. Jonak J, Karpiński R, Wójcik A. Numerical analysis of the effect of embedment depth on the geometry of the cone failure. *J Phys: Conf Ser*. 2021; 2130(1): 012012.
 48. Ferdynus M, Rogala M. Numerical crush analysis of thin-walled aluminium columns with square cross-section and a partial foam filling. *Adv Sci Technol Res J*. 2019; 13(3): 144–51.
 49. Kopecki T, Świąch Ł. Experimental-numerical analysis of a flat plate subjected to shearing and manufactured by incremental techniques. *Adv Sci Technol Res J*. 2023; 17(4): 179–88.
 50. Grzes P, Kuciej M. Coupled thermomechanical FE model of a railway disc brake for friction material wear calculations. *Wear*. 2023; 530–531: 205049.
 51. Świąch Ł. Experimental and numerical studies of low-profile, triangular grid-stiffened plates subjected to shear load in the post-critical states of deformation. *Materials*. 2019; 12(22): 3699.
 52. Świąch Ł. Finite element analysis of stress distribution in the node region of isogrid thin-walled panels. In: Mężyk A, Kciuk S, Szewczyk R, Duda S, (Eds.). *Modelling in Engineering 2020: Applied Mechanics [Internet]*. Cham: Springer International Publishing; 2021; 279–88. (*Advances in Intelligent Systems and Computing*; t. 1336). Available at: http://link.springer.com/10.1007/978-3-030-68455-6_25
 53. Wysmulski P, Falkowicz K, Filipek P. Buckling state analysis of compressed composite plates with cut-out. *Composite Structures*. 2021; 274: 114345.
 54. Falkowicz K, Wysmulski P, Debski H. Buckling analysis of laminated plates with asymmetric layup by approximation method. *Materials*. 2023; 16(14): 4948.
 55. Wysmulski P, Debski H, Falkowicz K. Sensitivity of compressed composite channel columns to eccentric loading. *Materials*. 2022; 15(19): 6938.
 56. Falkowicz K, Kulisz M. Prediction of buckling behaviour of composite plate element using artificial neural networks. *Adv Sci Technol Res J*. 2024; 18(1): 231–43.